Regular Octahedral Coordination of As(III) in the Anion $[As_3Br_{12}]^{3-}$ Structural Correlation of the Antibonding Influence of the As 4s-Orbital in Bromoarsenates(III)

W. S. Sheldrick* and C. Horn

Fachbereich Chemie der Universität Kaiserslautern, Erwin-Schrödinger-Straße, D-6750 Kaiserslautern

Z. Naturforsch. **44b**, 405–411 (1989); received November 7, 1988

Bromoarsenates(III), X-Ray, Structural Correlation, Bond Valences

The bromoarsenates(III) $[Et_4N]_3[As_3Br_{12}]$ (**1**), $[Ph_4P]_2[As_2Br_8]$ (**2**), $[(n\text{-prop})_4N]_2[As_2Br_8]$ (**3**) and $\{[pipH]_3[As_2Br_9]\cdot[pipH]Br\}$ (**4**) have been prepared and their structures established by X-ray structural analysis. The central As atom in the novel face-bridged trioctahedral species $[As_3Br_{12}]^{3-}$ displays an effectively regular octahedral coordination in one of the two independent anions in the unit cell of **1**. The As–Br distances are 2.671(1)–2.672(2) Å with Br–As–Br angles in the range 88.8(1)–91.2(1)°. In contrast the outer As atoms exhibit a severely distorted octahedral geometry with three short As–Br terminal bonds (2.404(2)–2.409(2) Å). The $[As_2Br_8]^{2-}$ anions in **2** and **3** are centrosymmetric with the As atoms displaying a square-pyramidal coordination. A structural correlation of opposite As–Br distances in the linear three-centre Br–As···Br interactions is presented. The sum of the bond valences in bromoarsenates(III) is a minimum for the regular octahedral geometry, reflecting, thereby, the influence of the As 4s-orbital in the antibonding $2a_{1g}$ MO. An empirical expression for As–Br distances in bromoarsenates(III) is derived.

Introduction

Weak interatomic contacts are characteristic for compounds of arsenic(III) in the solid state [1–3]. Such secondary bonds As···Y, which are frequently appreciably shorter than the van der Waals distance, tend to form in directions which are collinear with primary bonds As–X [4]. If these interactions are included, then coordination numbers of five and six have been established for all halogenoarsenate(III) anions studied by X-ray diffraction. These anions may be regarded as being derived from a hypothetical regular octahedral species AsX_6^{3-}, in which three facially positioned As–X bonds are subsequently stretched, accompanied by a concomitant shortening and strengthening of the opposite primary bonds. In the case of fivefold coordination one of the ligands is completely expelled from the coordination sphere leading to a distorted square pyramidal arrangement, in which the apical position is occupied by what is essentially an As–X single bond.

The structural chemistry of the analogous halogenoantimonates(III) has been extensively studied [5]. Several authors have attempted to correlate Sb–X primary bond distances with those of the *trans*-sited Sb···X secondary interactions using semiempirical bond-valence expressions of the form $s = (r/r_o)^{-N}$ or $s = \exp[(r_o - r)/B]$, where s is the bond valence for an Sb–X distance r and r_o and N or r_o and B are constants for a particular atom pair [5–7]. A theoretical justification based on the angular overlap model has recently been provided by Burdett [8] for the application of such expressions to two centre – two electron bonds. However, their implementation in the case of three centre X–A···X interactions (A = As(III), Sb(III)) can only be accepted if the assumption that the sum of the individual bond valencies around the central atom i, $\sum_j s_{ij}$, remains equal to the formal valency V_i (= 3) of this atom has validity. A simple qualitative molecular orbital approach [9] immediately indicates that this cannot be the case for the 14-electron species AsX_6^{3-} and SbX_6^{3-}. The occupied molecular orbitals for regular octahedral (O_h) symmetry may be classified as $1a_{1g}$ (bonding), $1t_{1u}$ (3 × bonding), e_g (2 × nonbonding) and $2a_{1g}$ (antibonding = HOMO). The LUMO displays t_{1u}-symmetry (antibonding). Thus, there are two completely symmetric MOs (a_{1g}) produced by in-phase or out-of-phase combinations of the central atom s orbital and the ligand AOs (Fig. 1). MO normalization requires that the antibonding $2a_{1g}$ orbital will make a greater contribution to the total bond order than the bonding $1a_{1g}$ orbital.

* Reprint requests to Prof. Dr. W. S. Sheldrick.

Verlag der Zeitschrift für Naturforschung, D-7400 Tübingen
0932–0776/89/0400–0405/$ 01.00/0

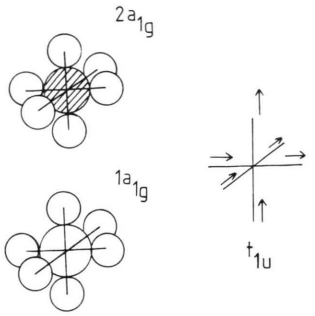

Fig. 1. (a) $1a_{1g}$ and $2a_{1g}$ (HOMO) orbitals for 14-electron AX_6 species; (b) t_{1u} stretching mode of octahedral AX_6 species.

Application of the second-order Jahn-Teller concept [10] indicates that 14-electron octahedral species will be unstable with respect to a distortion of t_{1u} symmetry, which allows mixing of the HOMO and LUMO orbitals leading to a stabilization of the former $2a_{1g}$ orbital. X-ray diffraction studies confirm that the t_{1u} stretching mode (Fig. 1) is preferred over the alternative t_{1u} bending mode by As(III) and Sb(III) halides in the solid state leading to the typical distorted octahedral geometry with three short and three long *trans*-sited A–X bonds. This approach demonstrates that there will be both an a_{1g} (net antibonding) and t_{1u} (bonding) MO contribution to the total bond order of A–X bonds in halogenoarsenates(III) and -antimonates(III), in which the central atom displays a formally octahedral geometry. As the latter bonding contribution will be relatively more effective at longer range owing to the more diffuse character of the *p*-orbitals involved, the observed distorted structure will be energetically favourable in comparison to a regular O_h-geometry. For the expected flat minimum, crystal forces will determine the experimental geometry.

Adoption of the three-centre approach of Rundle and Pimentel readily allows the extension of these ideas to geometries other than octahedral. Fig. 2 shows an MO diagram for symmetrical and asymmetric X–A–X species. The driving force for distortion is once again the loss of antibonding interaction in the $1\sigma_g^+$ orbital to be weighed against the loss of stabilization in the $1\sigma_u^+$ orbital.

In this work we present a full structural correlation for As–Br distances in bromoarsenates(III), which allows a metrical estimation of the antibonding influence of the As 4s-orbital. The energetic similarity of the As 4s- and the Br 4p-orbitals suggested a marked contribution of the former AO to the $1\sigma_g^+$ MOs. Crystal structures are presented for $[Et_4N]_3[As_3Br_{12}]$ (**1**), $[Ph_4P]_2[As_2Br_8]$ (**2**), $[(n\text{-prop})_4N]_2[As_2Br_8]$ (**3**) and $\{[pipH]_3[As_2Br_9]\cdot[pipH]Br\}$ (**4**). The central As atom in the novel face-bridged trioctahedral species $[As_3Br_{12}]^{3-}$ displays an almost perfect O_h-symmetry in one of two independent anions in the unit cell. This represents the first example of regular octahedral coordination for As(III) in a discrete anion characterized by diffraction methods.

Experimental

All preparations were performed under argon. In a typical synthesis 3 mmol of $AsBr_3$ in 5 ml of absolute CH_3CN were added to a suspension of 3 mmol of the bromide of the required cation in 12 ml

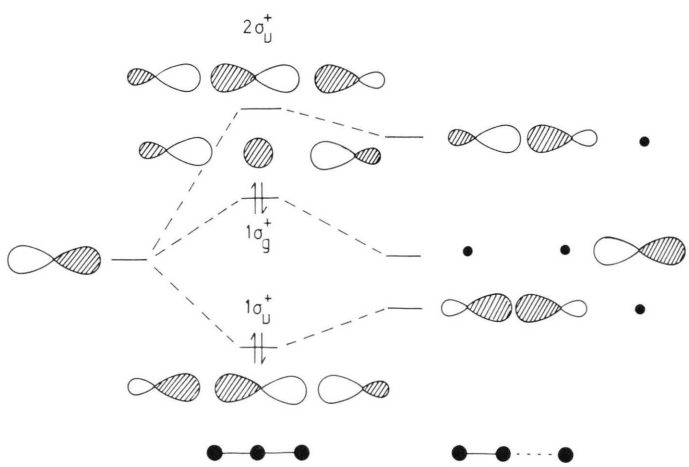

Fig. 2. MO diagram for symmetrical and asymmetric AX_2 species.

CH_3CN. The suspension was heated with stirring at reflux for 3d. After filtration at R.T. the resulting yellow solution was cooled slowly to −30 °C yield crystals of **1–4.** The given yields are based on $AsBr_3$.

$[Et_4N]_3[As_3Br_{12}]$ (**1**), *M = 1574.4 (yield 70%)*
Calcd C 18.31 H 3.84 N 2.67,
Found C 18.4 H 3.73 N 2.9.

$[Ph_4P]_2[As_2Br_8]$ (**2**), *M = 1467.9 (yield 82%)*
Calcd C 39.27 H 2.75,
Found C 39.0 H 2.76.

$[(n\text{-}prop)_4N]_2[As_2Br_8]$ (**3**), *M = 1161.8 (yield 72%)*
Calcd C 24.80 H 4.86 N 2.41,
Found C 24.6 H 4.71 N 2.4.

$\{[pipH]_3[As_2Br_9]\cdot[pipH]Br\}$ (**4**), *M = 1293.6 (yield 83%)*
Calcd C 18.50 H 3.74 N 4.33,
Found C 18.3 H 3.56 N 4.5 .

X-ray diffraction studies on **1–4**

Crystal and refinement data are presented in Table I. Reflection intensities were collected on an Enraf-Nonius CAD4 diffractometer. Empirical absorption corrections were applied. The structures were solved by direct methods (MULTAN-82) and refined by full-matrix least-squares. Hydrogen atoms at calculated positions were included in the final cycles for **2** and **3.** These atoms were assigned a joint isotropic temperature factor. The remaining atoms in **2** and **3** were refined anisotropically. Hydrogen atoms were not included in the final cycles for **1** and **4.** For these compounds only the anion As and Br atoms were assigned anisotropic temperature factors. Weights were given by $w = (\sigma^2(F_o) + p^2F_o^2)^{-1}$ with values of p listed in Table I. Positional parameters for the anion atoms As and Br in **1–4** are given in Table II, bond lengths and angles in the anions in Table III. For the sake of brevity the cation atoms are not included in Table II. Their positions have been deposited*.

Discussion

Anion structures of **1–4**

The crystal lattice of **1** contains two independent anions $[As_3Br_{12}]^{3-}$ of which the latter displays crystallographic C_1-symmetry. Both anions adopt the novel face-bridged trioctahedral arrangement depicted in Fig. 3. All six As5–Br distances are equivalent (2.671(2), 2.671(1), 2.672(2) Å) for the central atom

* Further details of the crystal structure analyses may be obtained from Fachinformationszentrum Energie, Physik, Mathematik, D-7514 Eggenstein-Leopoldshafen 2, upon specification of the deposition number CSD 53698, the authors and the journal reference.

Table I. Crystal and refinement data for **1–4.**

Compound	**1**	**2**	**3**	**4**
Crystal system	Triclinic	Triclinic	Orthorhombic	Monoclinic
Space group	$P\bar{1}$	$P\bar{1}$	*Pbca*	$P2_1/c$
a (Å)	17.705(5)	11.085(3)	15.206(3)	9.823(1)
b (Å)	17.774(7)	12.300(3)	13.559(2)	19.494(3)
c (Å)	14.259(3)	10.605(5)	19.500(3)	20.568(2)
α (°)	102.30(4)	112.39(3)	90	90
β (°)	102.56(4)	91.69(3)	90	90.74(2)
γ (°)	118.37(1)	102.23(2)	90	90
Z	3	1	4	4
M	1574.4	1467.9	1161.8	1293.6
D_{calc} ($g\cdot cm^{-3}$)	2.19	1.88	1.92	2.18
Radiation	CuK_α	CuK_α	CuK_α	MoK_α
Crystal size (mm)	0.48×0.48×0.32	0.58×0.48×0.28	0.31×0.23×0.22	0.40×0.36×0.28
μ (cm^{-1})	146.2	97.7	116.5	117.6
2θ-range	$2\theta \leq 115°$	$2\theta \leq 140°$	$2\theta \leq 120°$	$2\theta \leq 45°$
Scan method	$\theta-2\theta$	ω	$\theta-2\theta$	ω
Reflections collected	9792	4704	2992	5185
Reflections observed	7692	4486	2161	2138
Observation criterion	$F_o^2 \geq 1.5\sigma(F_o^2)$	$F_o^2 \geq 1.0\sigma(F_o^2)$	$F_o^2 \geq 2.0\sigma(F_o^2)$	$F_o^2 \geq 1.5\sigma(F_o^2)$
R	0.076	0.047	0.047	0.072
R_w	0.076	0.048	0.045	0.063
p-	0.010	0.002	0.005	0.020

Table II. Positional parameters with equivalent isotropic temperature factors for the anion atoms in **1–4.**

Atom	*x/a*	*x/b*	*z/c*	U_{eq}
1 $[As_3Br_{12}]^{3-}$				
Br1	0.4199(1)	0.1986(2)	0.6183(1)	0.077(1)
Br2	0.6453(1)	0.3294(1)	0.6135(1)	0.073(1)
Br3	0.5555(2)	0.1023(1)	0.6113(2)	0.085(1)
Br4	0.5202(1)	0.1694(1)	0.8774(1)	0.054(1)
Br5	0.6131(1)	0.4098(1)	0.8763(1)	0.051(1)
Br6	0.7600(1)	0.3120(1)	0.8790(1)	0.054(1)
Br7	0.8087(1)	0.5079(1)	0.1186(1)	0.056(1)
Br8	0.7474(1)	0.2785(1)	0.1219(1)	0.056(1)
Br9	0.5785(1)	0.3473(1)	1.1205(1)	0.057(1)
Br10	0.6981(2)	0.3474(2)	1.3913(2)	0.097(1)
Br11	0.7730(2)	0.5690(2)	1.3840(2)	0.089(1)
Br12	0.9215(1)	0.4860(2)	0.3888(2)	0.085(1)
Br13	1.1603(2)	0.2493(1)	1.3924(1)	0.083(1)
Br14	−0.0024(1)	0.0301(1)	0.3867(1)	0.079(1)
Br15	0.2174(1)	0.0825(2)	0.3884(2)	0.084(1)
Br16	0.1765(1)	0.1247(1)	0.1234(1)	0.054(1)
Br17	0.9505(1)	0.0894(1)	0.1222(1)	0.052(1)
Br18	0.9916(1)	0.9006(1)	1.1186(1)	0.052(1)
As1	0.5735(1)	0.2415(1)	0.7122(1)	0.046(1)
As2	0.6731(1)	0.3388(1)	1.0016(1)	0.041(1)
As3	0.7651(1)	0.4342(1)	1.2913(1)	0.052(1)
As4	1.0940(1)	0.0907(1)	1.2914(1)	0.050(1)
As5	0.0	0.0	0.0	0.044(1)
2 $[As_2Br_8]^{2-}$				
Br1	0.9473(1)	−0.2800(1)	0.5110(1)	0.066(1)
Br2	0.9792(1)	−0.3373(1)	0.1598(1)	0.060(1)
Br3	0.6910(1)	−0.3008(1)	0.2858(1)	0.063(1)
Br4	1.1529(1)	−0.0243(1)	0.4258(1)	0.055(1)
As1	0.9108(1)	−0.1933(1)	0.3566(1)	0.040(1)
3 $[As_2Br_8]^{2-}$				
Br1	0.6751(1)	0.3905(1)	0.5663(1)	0.056(1)
Br2	0.7326(1)	0.6431(1)	0.5666(1)	0.073(1)
Br3	0.5951(1)	0.5467(1)	0.7008(1)	0.054(1)
Br4	0.5845(1)	0.5521(1)	0.4309(1)	0.049(1)
As1	0.6033(1)	0.5422(1)	0.5708(1)	0.036(1)
4 $[As_2Br_9]^{3-} \cdot Br^-$				
Br1	0.3741(3)	0.0553(2)	0.8310(2)	0.077(3)
Br2	0.1859(3)	0.1468(2)	0.7117(1)	0.064(2)
Br3	0.0050(3)	0.0540(2)	0.8348(2)	0.071(2)
Br4	0.3898(4)	0.3135(2)	1.0181(2)	0.087(3)
Br5	0.0287(4)	0.3170(2)	1.0245(2)	0.084(3)
Br6	0.2068(4)	0.4169(2)	0.9074(2)	0.097(3)
Br7	−0.0097(3)	0.2555(2)	0.8413(2)	0.066(2)
Br8	0.2030(3)	0.1479(2)	0.9704(1)	0.061(2)
Br9	0.3835(3)	0.2499(2)	0.8353(2)	0.064(2)
Br10	0.8407(4)	0.1826(2)	0.1635(2)	0.100(3)
As1	0.1986(3)	0.1412(1)	0.8326(1)	0.049(2)
As2	0.2041(3)	0.2982(2)	0.9451(2)	0.053(2)

Table III. Bond lengths and angles in the anions of **1–4.**

1 $[As_3Br_{12}]^{3-}$			
As1–Br1	2.405(2)	As3–Br9	3.046(2)
As1–Br2	2.422(2)	As3–Br10	2.398(3)
As1–Br3	2.414(2)	As3–Br11	2.400(3)
As1–Br4	3.030(2)	As3–Br12	2.410(2)
As1–Br5	3.037(2)	As4–Br13	2.406(2)
As1–Br6	3.084(2)	As4–Br14	2.409(2)
As2–Br4	2.725(2)	As4–Br15	2.404(2)
As2–Br5	2.706(2)	As4–Br16	3.088(2)
As2–Br6	2.676(2)	As4–Br17	3.087(2)
As2–Br7	2.616(2)	As4–Br18	3.076(2)
As2–Br8	2.638(2)	As5–Br16	2.671(1)
As2–Br9	2.658(2)	As5–Br17	2.672(2)
As3–Br7	3.101(2)	As5–Br18	2.671(2)
As3–Br8	3.097(2)		
Br2–As1–Br1	95.2(1)	Br10–As3–Br8	98.3(1)
Br3–As1–Br1	95.1(1)	Br11–As3–Br8	164.2(1)
Br4–As1–Br1	93.7(1)	Br12–As3–Br8	91.2(1)
Br5–As1–Br1	93.0(1)	Br10–As3–Br9	93.1(1)
Br6–As1–Br1	165.9(1)	Br11–As3–Br9	96.4(1)
Br3–As1–Br2	94.7(1)	Br12–As3–Br9	164.6(1)
Br4–As1–Br2	167.0(1)	Br11–As3–Br10	95.1(1)
Br5–As1–Br2	92.9(1)	Br12–As3–Br10	94.9(1)
Br6–As1–Br2	93.6(1)	Br12–As3–Br11	95.9(1)
Br4–As1–Br3	94.0(1)	Br14–As4–Br13	94.9(1)
Br5–As1–Br3	168.4(1)	Br15–As4–Br13	95.1(1)
Br6–As1–Br3	95.1(1)	Br16–As4–Br13	97.1(1)
Br5–As1–Br4	77.2(1)	Br17–As4–Br13	91.8(1)
Br6–As1–Br4	76.0(1)	Br18–As4–Br13	165.8(1)
Br6–As1–Br5	75.6(1)	Br15–As4–Br14	94.6(1)
Br5–As2–Br4	88.3(1)	Br16–As4–Br14	165.6(1)
Br6–As2–Br4	88.3(1)	Br17–As4–Br14	97.2(1)
Br7–As2–Br4	174.0(1)	Br18–As4–Br14	92.0(1)
Br8–As2–Br4	95.3(1)	Br16–As4–Br15	92.2(1)
Br9–As2–Br4	87.1(1)	Br17–As4–Br15	165.7(1)
Br6–As2–Br5	88.3(1)	Br18–As4–Br15	96.7(1)
Br7–As2–Br5	87.1(1)	Br17–As4–Br16	74.5(1)
Br8–As2–Br5	174.4(1)	Br18–As4–Br16	74.6(1)
Br9–As2–Br5	95.1(1)	Br18–As4–Br17	74.9(1)
Br7–As2–Br6	95.5(1)	Br17–As5–Br16	88.8(1)
Br8–As2–Br6	87.4(1)	Br18–As5–Br16	88.8(1)
Br9–As2–Br6	174.1(1)	Br18–As5–Br17	89.1(1)
Br8–As2–Br7	89.6(1)	As2–Br4–As1	81.0(1)
Br9–As2–Br7	89.5(1)	As2–Br5–As1	81.2(1)
Br9–As2–Br8	89.5(1)	As2–Br6–As1	80.8(1)
Br8–As3–Br7	73.3(1)	As3–Br7–As2	81.5(1)
Br9–As3–Br7	74.3(1)	As3–Br8–As2	81.2(1)
Br10–As3–Br7	166.2(1)	As3–Br9–As2	81.9(1)
Br11–As3–Br7	91.8(1)	As5–Br16–As4	81.5(1)
Br12–As3–Br7	96.1(1)	As5–Br17–As4	81.5(1)
Br9–As3–Br8	74.7(1)	As5–Br18–As4	81.7(1)
2 $[As_2Br_8]^{2-}$			
As1–Br1	2.366(1)	As1–Br2	2.431(1)
As1–Br3	2.454(1)	As1–Br4	2.901(1)
As1–Br4′	3.030(1)		
Br1–As1–Br2	96.62(1)	Br1–As1–Br3	95.96(1)
Br1–As1–Br4	95.40(1)	Br1–As1–Br4′	93.85(1)
Br2–As1–Br4	91.71(1)	Br2–As1–Br4′	167.66(1)
Br3–As1–Br4	167.02(1)	Br3–As1–Br4′	92.22(1)
Br4–As1–Br4′	80.78(1)	Br2–As1–Br3	93.18(1)

Table III (continued).

3 $[As_2Br_8]^{2-}$			
As1–Br1	2.335(1)	As1–Br2	2.400(1)
As1–Br3	2.546(1)	As1–Br4	2.753(1)
As1–Br4′	3.134(1)		
Br1–As1–Br2	96.87(3)	Br1–As1–Br3	94.67(3)
Br1–As1–Br4	93.75(3)	Br1–As1–Br4′	93.14(3)
Br2–As1–Br4	91.35(3)	Br2–As1–Br4′	168.97(3)
Br3–As1–Br4	170.26(3)	Br3–As1–Br4′	88.58(3)
Br4–As1–Br4′	85.11(3)	Br2–As1–Br3	93.48(3)
4 $[As_2Br_9]^{3-}$			
As1–Br1	2.404(4)	As2–Br4	2.377(4)
As1–Br2	2.490(4)	As2–Br5	2.418(5)
As1–Br3	2.552(4)	As2–Br6	2.439(4)
As1–Br7	3.030(4)	As2–Br7	3.090(4)
As1–Br8	2.837(4)	As2–Br8	2.977(4)
As1–Br9	2.791(4)	As2–Br9	3.032(5)
Br2–As1–Br1	92.5(2)	Br6–As2–Br5	94.7(2)
Br3–As1–Br1	94.0(1)	Br7–As2–Br5	91.3(1)
Br7–As1–Br1	175.9(2)	Br8–As2–Br5	91.5(1)
Br8–As1–Br1	92.5(1)	Br9–As2–Br5	167.5(2)
Br9–As1–Br1	93.6(1)	Br7–As2–Br6	92.7(1)
Br3–As1–Br2	91.1(1)	Br8–As2–Br6	171.5(2)
Br7–As1–Br2	90.1(1)	Br9–As2–Br6	92.8(2)
Br8–As1–Br2	174.5(2)	Br8–As1–Br7	84.8(1)
Br9–As1–Br2	90.6(1)	Br8–As2–Br7	81.4(1)
Br7–As1–Br3	89.1(1)	Br9–As1–Br7	83.2(1)
Br8–As1–Br3	90.8(1)	Br9–As2–Br7	78.3(1)
Br9–As1–Br3	172.1(2)	Br9–As1–Br8	86.8(1)
Br5–As2–Br4	95.6(2)	Br9–As2–Br8	80.1(1)
Br6–As2–Br4	94.2(2)	As2–Br7–As1	77.6(1)
Br7–As2–Br4	169.8(2)	As2–Br8–As1	82.5(1)
Br8–As2–Br4	90.9(1)	As2–Br9–As1	82.3(1)
Br9–As2–Br4	93.8(1)		

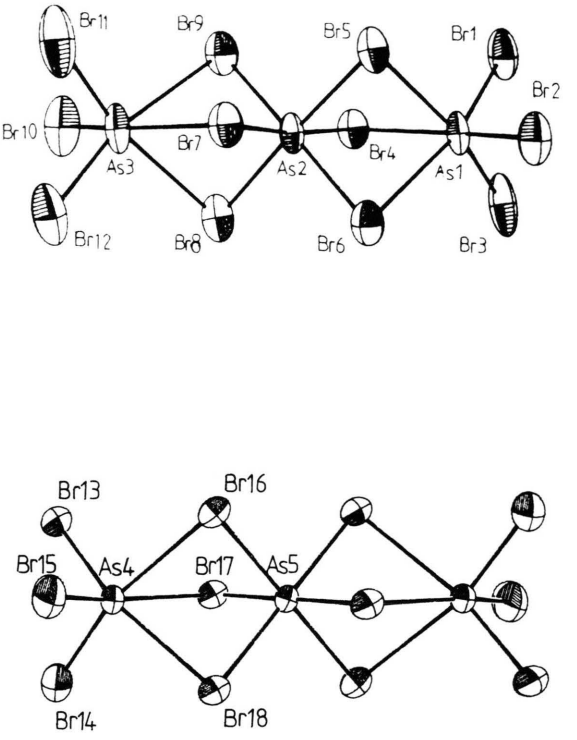

Fig. 3. The two independent trioctahedral $[As_3Br_{12}]^{3-}$ anions in **1.**

of the second centrosymmetric $[As_3Br_{12}]^{3-}$ anion. Only minor deviations from a perfect octahedral arrangement are observed for the Br–As5–Br angles; those for the bridging faces lie in the range 88.8(1)–89.1(1)°. This is the first example of an effectively regular octahedral coordination of As(III) in a discrete anion which has been established by X-ray diffraction for the solid state. In contrast to As5 the outer symmetry-related arsenic atoms As4 display the strongly t_{1u}-distorted octahedral arrangement typical for As(III) compounds with three short terminal As4–Br and three long bridging As4···Br bonds. The former bonds are only 0.075–0.092 Å longer than the As–Br single bond distance of 2.33 Å found for $AsBr_3$ in the gas phase [11].

Similar geometrical arrangements are also observed for the arsenic atoms As1–As3 in the first independent $[As_3Br_{12}]^{3-}$ anion. However, in this case, small but significant differences are found for the *trans*-related As2–Br bonds to the central atom. As discussed in the Introduction, an O_h-geometry must represent an energy maximum for As(III) in species AsX_6^{3-}, which will, therefore, be expected to display a t_{1u}-distortion. In this context, it is therefore appropriate to pose the question as to whether the regular octahedral coordination determined by X-ray structural analysis for As5 is, indeed, that of individual anions in the crystal lattice or whether it is rather the net result of a disordered occupation of this site by anions with a central geometry similar to that of As2 in the first anion. It is not possible to provide an unequivocal answer. However, the observation of very similar equivalent isotropic temperature factors for the atoms of the central $AsBr_6$ polyhedra in both anions provides experimental support for the former interpretation.

It is interesting to note that we have previously characterized a different trioctahedral $[As_3Br_{12}]^{3-}$ anion in the salt $[Et_3NH]_3[As_3Br_{12}]$ [12]. In the case a central $AsBr_6$ octahedron is connected *via* two faces with a common corner to two further $AsBr_6$ octahe-

dra. The bond distances to the central As atom lie between 2.483 and 2.862 Å. The observation of different anion species reflects the structural influence of cations in the halogenoarsenates(III).

Centrosymmetric anions $[As_2Br_8]^{2-}$ are found for both **2** and **3** (Fig. 4). The difference between the *trans*-related As1–Br3 and As1–Br4 distances is markedly smaller in **3** (0.207 Å) than in **2** (0.447 Å). We had hoped that the piperidinium salt **4** would contain the $[AsBr_5]^{2-}$ anion. However, the X-ray structural analysis revealed the presence of $[As_2Br_9]^{3-}$ and Br^- anions in a 1:1 ratio. The structure of the $[As_2Br_9]^{3-}$ anion is depicted in Fig. 5.

Structural correlation

The results of the present investigation taken together with our previous structural studies on [pyH][$AsBr_4$], [pyH]$_3$[As_2Br_9], [NmaH]$_2$[As_2Br_8] (Nma = N-methylaniline) [2], [Et_3NH]$_3$[As_3Br_{12}] [12] and [Me_4N]$_3$[As_2Br_9] [13] provide a total of 46 three-centre Br^1–As(III)–Br^2 interactions. A graphical structural correlation of opposite Br^1–As(r_1) and Br^2–As(r_2) distances is provided in Fig. 6. It is immediately apparent that, as discussed in the Introduction, Br–As distances in symmetrical or nearly symmetrical three-centre interactions (*e.g.* in **1** or in [pyH][$AsBr_4$]) are markedly longer than would be predicted by bond-valence expressions such as $r_n = r_o - B\ln s_n$ upon the assumption that the sum of the bond valencies s_1+s_2 remains constant at one. In this case the r_1 and r_2 values should be represented by hyperbolic function of the form $(r_1-r_o)(r_2-r_o) = C$, where r_o is 2.33 Å, the value of the As–Br single bond distance for $AsBr_3$ in the gas phase [11] and C is a constant (curve 1).

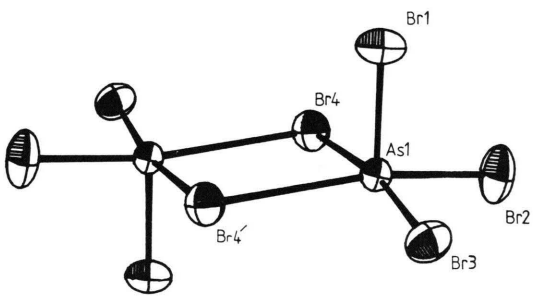

Fig. 4. The $[As_2Br_8]^{2-}$ anion in **3.** A similar numbering scheme is used for the analogous anion in **2.**

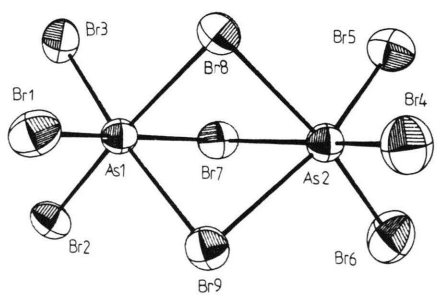

Fig. 5. The $[As_2Br_9]^{3-}$ anion in **4.**

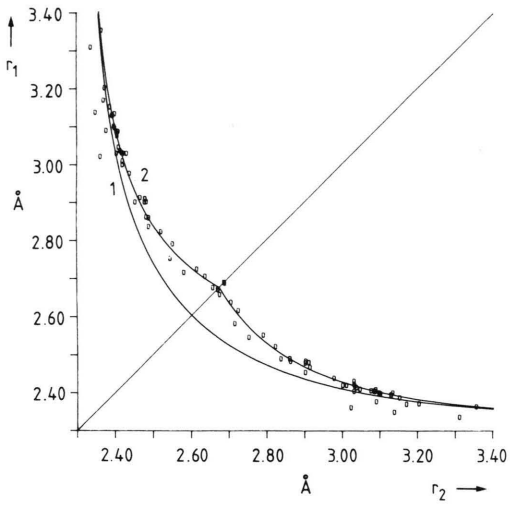

Fig. 6. Structural correlation of *trans*-related As–Br bond lengths in bromoarsenates(III).

An alternative way of demonstrating the reduction in the total bond valence for the three-centre Br^1–As–Br^2 bonds, as r_1 increases from r_o to equal r_2, is to calculate individual values of B for each example upon the assumption that $s_1+s_2 = 1$. As may be seen in Fig. 7 for 40 Br–As–Br interactions with $r_1-r_o \geq 0.05$ Å ($r_1 \leq r_2$), B increases steadily with the difference r_1-r_o, in order to compensate for the antibonding contribution of the $1\sigma_g^+$ orbital (Fig. 2), which reaches a maximum for the symmetrical arrangement with $r_1=r_2$. Six opposite As–Br bond pairs included in Fig. 6 with r_1-r_o values less than 0.05 Å were not used in this analysis, as the wide scatter of r_2 values observed for the extremely weak secondary bonds falsifies the observed trend. A correlation coefficient of 0.946 is obtained for the least squares line

$$B = B_o + A(r_1-r_o) \qquad (1)$$

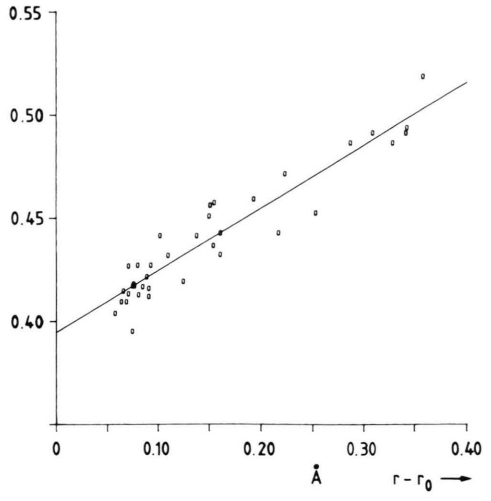

Fig. 7. Variation of B for the expression $r_o - r_n = B \ln s_n$ applied to *trans*-related As–Br bond lengths $r_n = r_1$ or r_2 in bromoarsenates(III) upon the assumption that the total bond order $s_1 + s_2$ for a three centre $Br^1-As\cdots Br^2$ interaction remains constant at 1.

where $B_o = 0.395$ ($r_1 = r_o$) and $A = 0.303$. In this context, it is interesting to note that one pair of opposite As–Br distances of 2.688(1) and 2.690(1) Å, very close to those observed for As5 in **1** is also found for the polymeric anion in [pyH][$AsBr_4$]. In contrast, the other pairs in the $[AsBr_4^-]_n$ anion are strongly distorted (2.393(1) and 2.395(1) opposite to 3.130(1) and 3.129(1) Å). This and other examples provide ample justification for the analysis of isolated three-centre bonds presented in this work.

Our results suggest that it is possible to modify the semiempirical bond-valence expression $r_n = r_o - B \ln s_n$ to allow for the antibonding contribution to Br–As–Br three-centre bonds involving the As 4s-orbital. An approximate empirical description of bond distances in bromoarsenates(III) is provided by the expression

$$r_n = r_o - [B_o + A(r_1 - r_o)] \ln s_n' \qquad (2)$$

for $r_1 \leq r_2$ and $s_1' + s_2' = 1$. The r_1 and r_2 distances calculated using equation 2 are given by curve 2 in Fig. 6. Curve 1 gives the As–Br distances predicted by the expression $r_n = r_o - B_o \ln s_n$. Inspection of Figs 6 and 7 indicates that the majority of Br–As–Br three-centre bonds in bromoarsenates(III) are extremely asymmetric with $r_1 - r_o$ in the range 0.05–0.20 Å and B between 0.40 and 0.45. Symmetrical three-centre bonds represent an energy maximum which must be compensated for by crystal forces in the lattices of $[Et_4N]_3[As_3Br_{12}]$ or [pyH][$AsBr_4$]. For A=0 in equation 2 a value of 2.604 Å would be expected for a symmetrical Br–As–Br three-centre bond involving alone a central As 4p-orbital. The observed values for such interactions of 2.671–2.672 Å in **1** and 2.689 Å (average) in [pyH][$AsBr_4$] reflect the net antibonding influence of the As 4s-orbital (*i.e.* $2a_1$ antibonding MO minus a_1 bonding MO). A comparison of the Sb–Br distances of respectively 2.564 and 2.795 Å in the 12 and 14 electron species $SbBr_6^-$ and $SbBr_6^{3-}$ [14] provides a direct measure of the $2a_1$ antibonding contribution for antimony. Our results for bromoarsenates(III) demonstrate that the arsenic 4s-orbital is stereochemically active in the sense that it leads to the characteristic t_{1u} distortion of octahedrally coordinated As(III) species. Curve 2 provides a semiempirical measure of the net antibonding contribution of this orbital for a particular geometry.

[1] J. Kaub and W. S. Sheldrick, Z. Naturforsch. **39b,** 1252 (1984).
[2] J. Kaub and W. S. Sheldrick, Z. Naturforsch. **39b,** 1257 (1984).
[3] W. S. Sheldrick, H.-J. Häusler, and J. Kaub, Z. Naturforsch. **43b,** 789 (1988).
[4] N. W. Alcock, Adv. Inorg. Chem. Radiochem. **15,** 1 (1972).
[5] I. D. Brown, J. Solid State Chem. **11,** 214 (1974).
[6] A. Lipka, Z. Kristallogr. **158,** 88 (1982).
[7] J. F. Sawyer and R. J. Gillespie, Progr. Inorg. Chem. **34,** 65 (1986).
[8] J. K. Burdett, Chem. Rev. **88,** 3 (1988).
[9] B. M. Gimarc, Molecular Structure and Bonding – The Qualitative Molecular Orbital Approach, Academic Press, New York, pp. 71 (1979).
[10] L. S. Bartell, J. Chem. Educ. **45,** 754 (1968).
[11] Y. Morino, K. Kuchitsu, and T. Moritani, Inorg. Chem. **8,** 867 (1969).
[12] W. S. Sheldrick and H.-J. Häusler, Angew. Chem. **99,** 1184 (1987).
[13] W. S. Sheldrick and C. Horn, unpublished results.
[14] S. L. Lawton and R. A. Jacobson, J. Am. Chem. Soc. **88,** 616 (1966).